Investigating the theoretical optical properties of neutral Cycloparaphenylenes (CPPs)

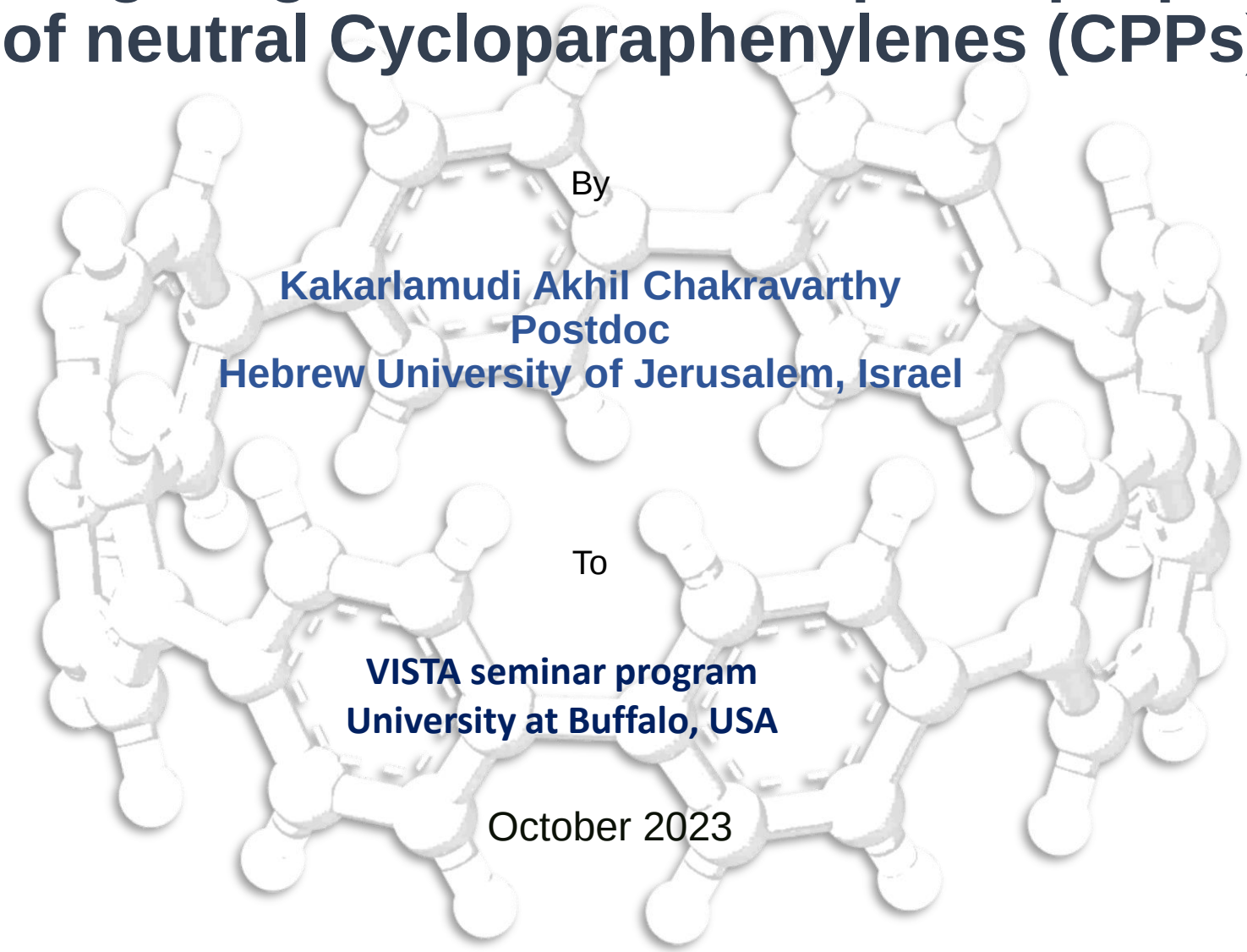

By

Kakarlamudi Akhil Chakravarthy
Postdoc
Hebrew University of Jerusalem, Israel

To

VISTA seminar program
University at Buffalo, USA

October 2023

Introduction

- In 1934 Perekh and Guha first attempt to make the smallest and simplest form of Cycloparaphenylenes(CPP) [a]

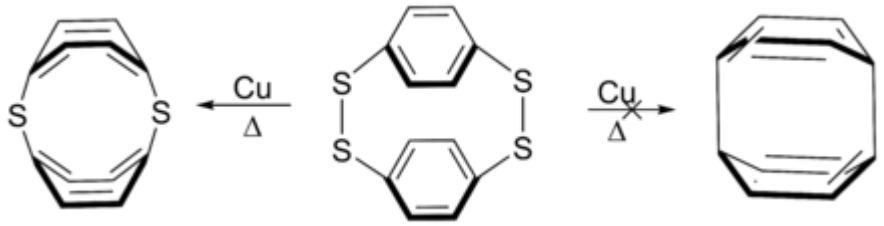

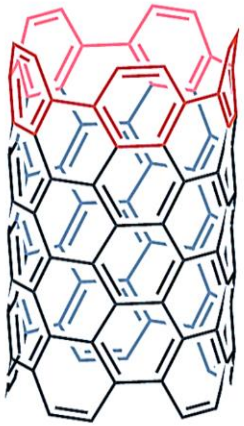

[5,5]CNT

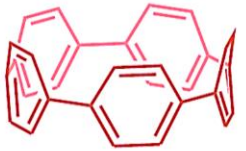

[5]CPP

- In 1993, Fritz Vögtle “On The Way to Macrocyclic Paraphenylenes” [b]
- In 2000, computational work done by Chandrasekhar, et al [c]
- First CPPs were synthesized by Ramesh Jasti and Carolyn R. Bertozzi group in 2008 [d]
- CPPs are cylindrical molecules made of para-linked benzene rings in a hoop-like structure [d]
- Internal conversion and intersystem crossing processes in singlet–triplet photophysics is essential for designing efficient photoluminescent molecular systems[e]

a. V. C. Parekh and P. C. Guha, J. Indian Chem. Soc., 11, 95, 1934
b. R. Friederich, M. Nieger and F. Vögtle, Chem. Ber., 126, 1723, 1993
c. Chandrasekhar, et al., Molecular Modeling Annual. 6,226–233, 2000
d. R. Jasti, J. Bhattacharjee, J. B. Neaton and C. R. Bertozzi, J. Am. Chem. Soc., 130, 17646, 2008
e. V. S. Reddy, C. Camacho, J. Xia, R. Jasti, and S. Irle J. Chem. Theory Comput. 13, 10, 4944,.2017

Applications

Carbon nanotubes [a]

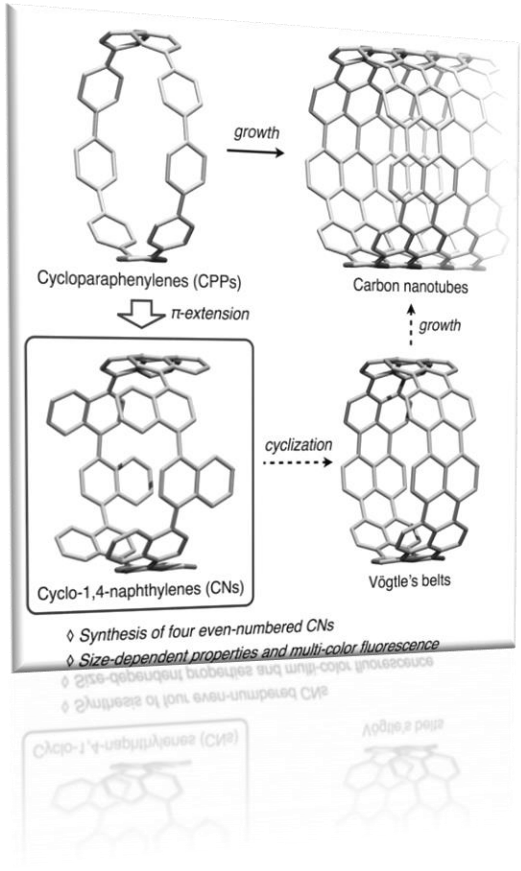

Unique ionic supra-molecular nanocarbons [b]

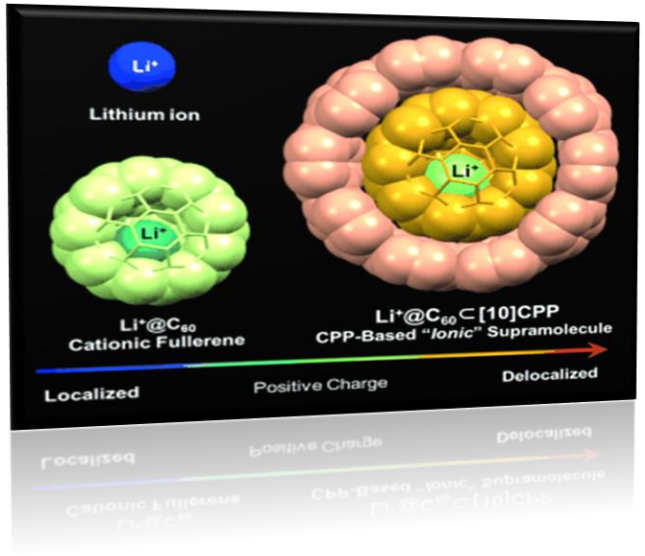

Live cell imaging [d]

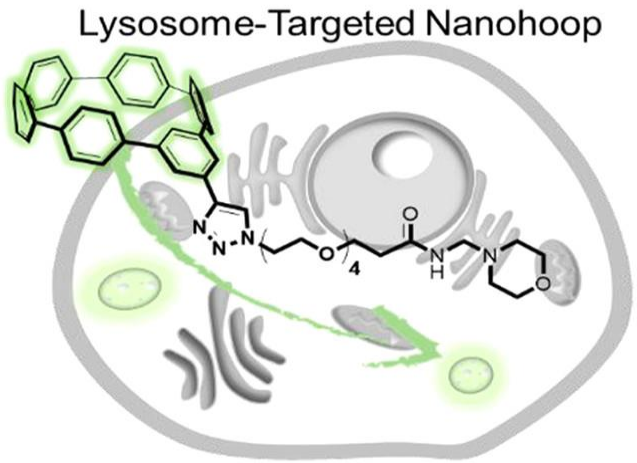

Electric stimuli [c]

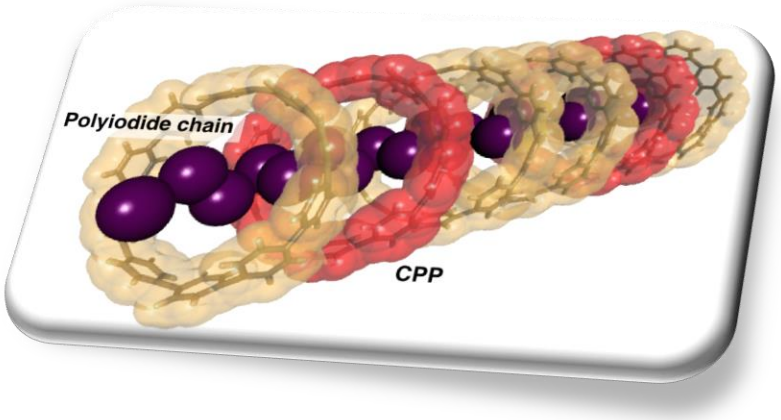

Polymerization [e]

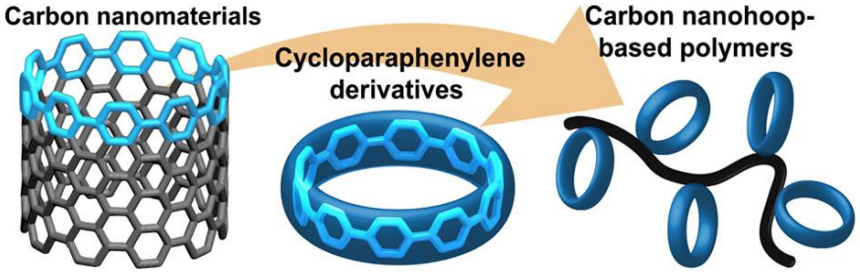

a. Y. Nakanishi, H. Omachi, S. Matsuura, Y. Miyata, R. Kitaura, Y. Segawa, K. Itami, H. Shinohara, Angew. Chem. Int. Ed. 53, 3102 ,2014
b. H.Ueno,T. Nishihara. Y Segawa, and K. Itami Angew. Chem. Int. Ed. 54, 3707, 2015
c. N. Ozaki, H. Sakamoto, T. Nishihara, T Fujimori, Y. Hijikata, R. Kimura, S. Irle, and K. Itami. Angew. Chem. Int. Ed. 56, 11196, 2017
d. T. C. Lovell, S. G. Bolton, J. P. Kenison, J. Shangguan, C. E. Otteson, F. Civitci, X Nan, M. D. Pluth, and R. Jasti ACS Nano 15 (9), 15285, 2021
e. R. L. Maust, P. Li, B. Shao, S. M. Zeitler, P. B. Sun, H. W. Reid , L. N. Zakharov, M. R. Golder, and R. Jasti ACS Cent. Sci. 7, 6, 1056, 2021

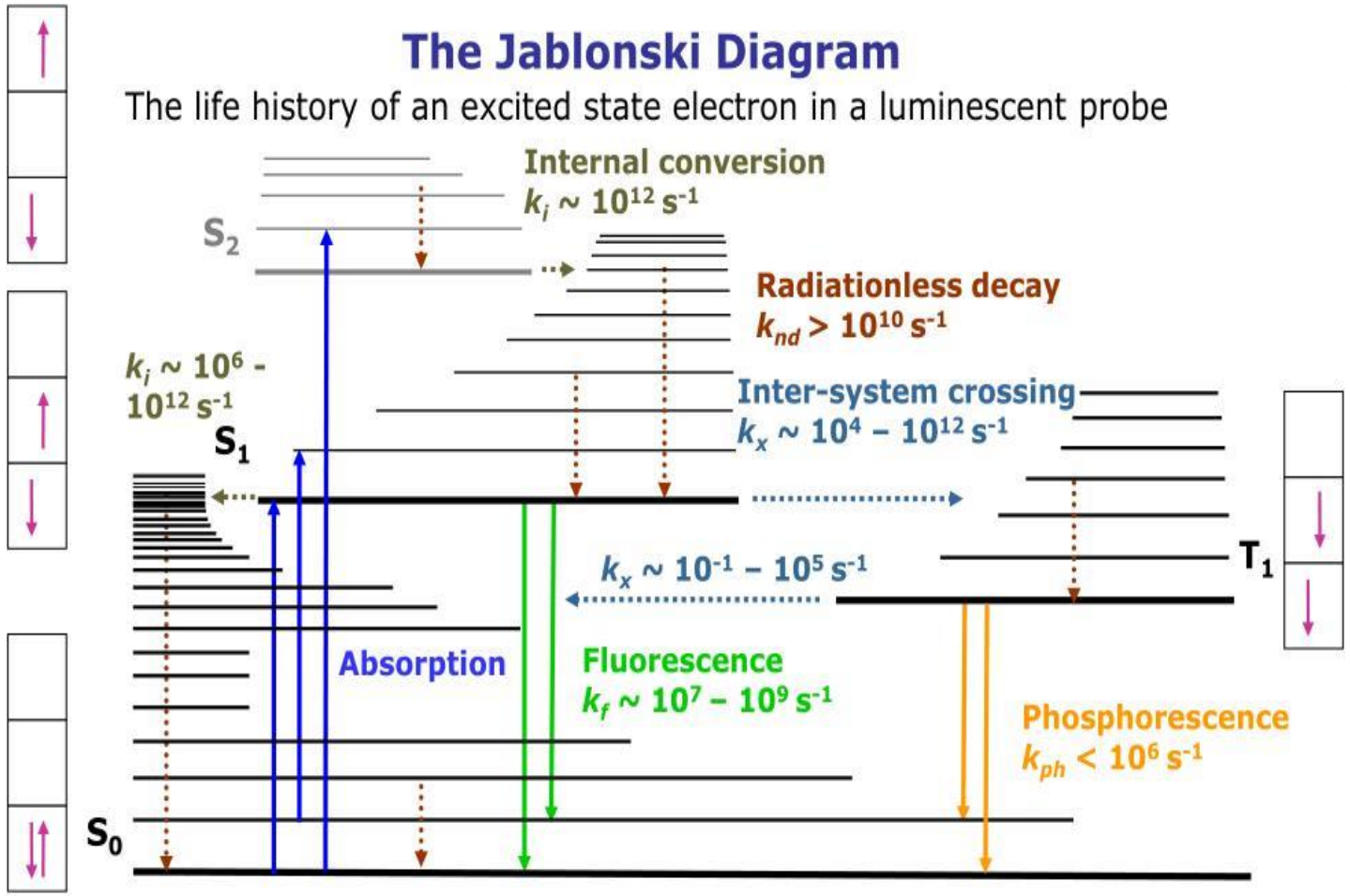

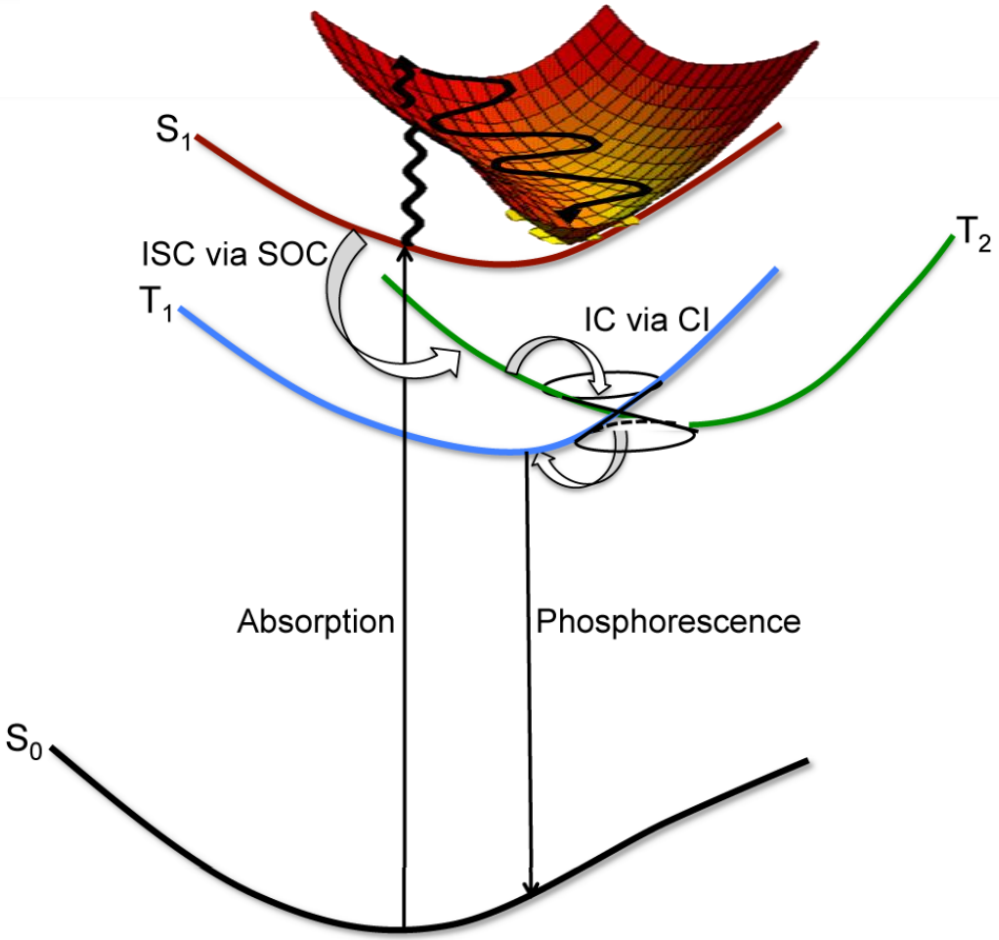

Pic credits: Edinburgh Instruments website
J. E. Subotnik, E. C. Alguire, Q. Ou, and B. R. Landry Acc. Chem. Res. 48, 1340, 2015

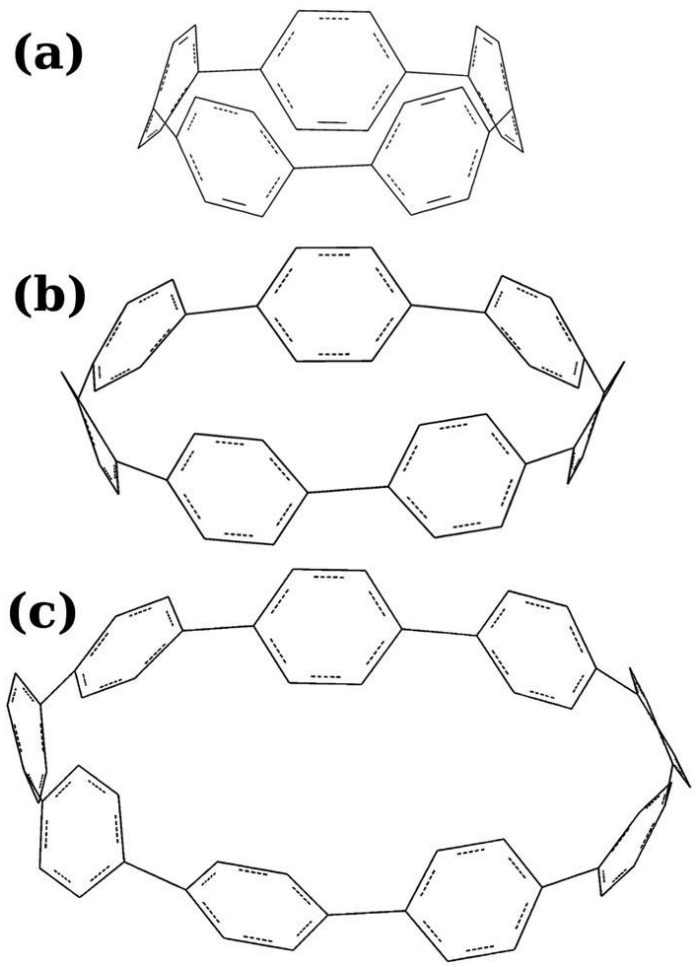

FIG. 1. Molecular structure of (a) [5]CPP (b) [7]CPP, and (c) [9]CPP.

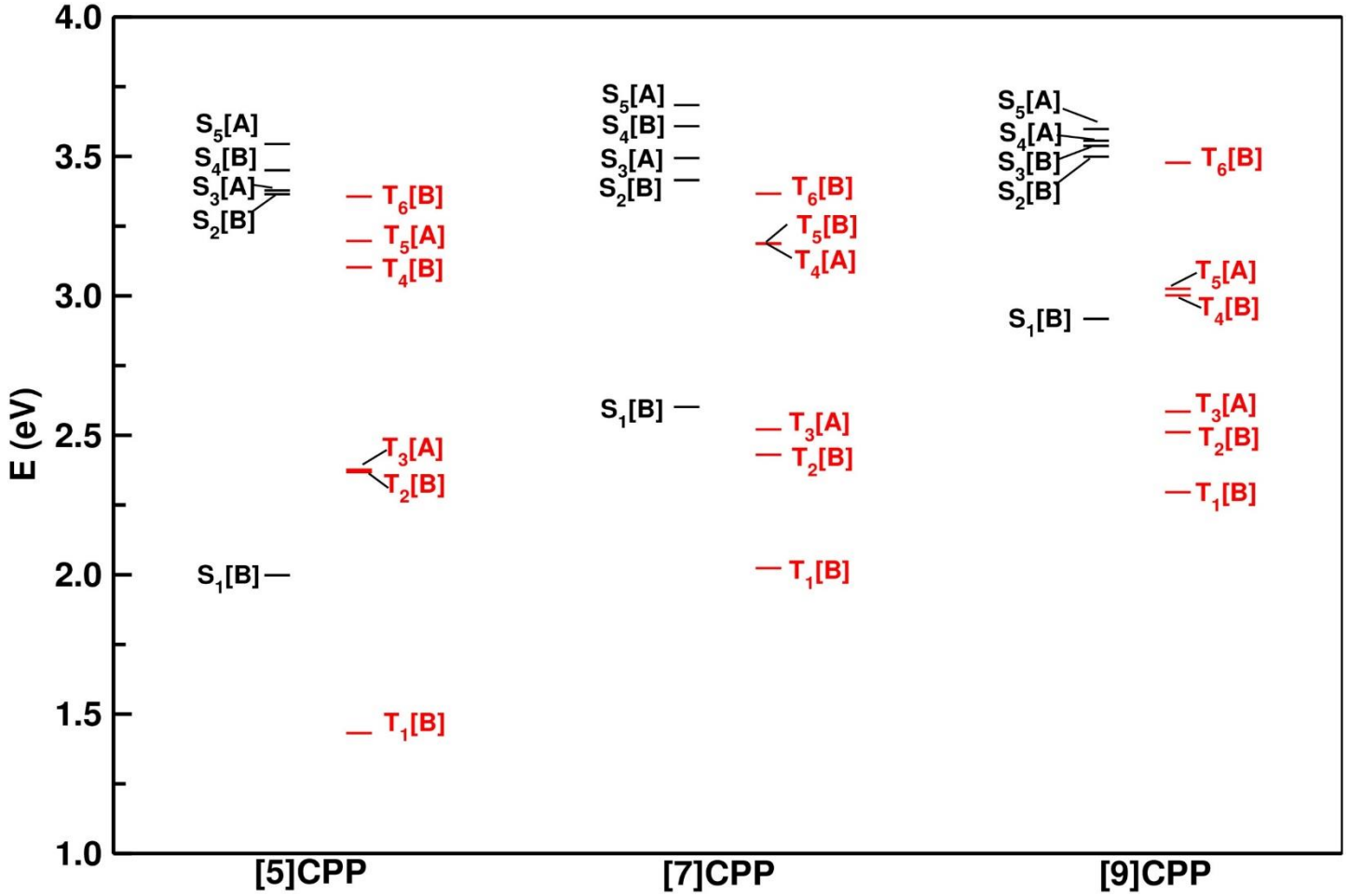

FIG. 2. FC vertical excitation energies of low-lying excited states of [5]-, [7]-, and [9]CPP computed with C_2 symmetry point group constraints using the TD-B3LYP/6-311G(d) level of theory.

A.C. Kakarlamudi and S.R. Vennapusa J. Chem. Phys.,155, 044301, 2021

TABLE 1. Vertical excitation energies (in eV) of singlet excited-states and corresponding oscillator strength(parenthesis) of [5]-, [7]- and [9]CPP. Experimental absorption maximum of S_1 band of CPPs also given.

[n]CPP	state	TD-B3LYP/6-311g(d)	ADC(2)/cc-pVDZ	CASSCF/cc-pVDZ	Expt.
[5]CPP	S_1	2.01(0.00)	2.57(0.00)	2.59(0.00)	2.47[a]
	S_2	3.37(0.00)	3.83(0.02)	3.73(0.00)	
	S_3	3.39(0.01)	3.95(0.04)	3.95(0.01)	
	S_4	3.46(0.00)	4.15(0.05)	3.95(1.51)	
	S_5	3.55(0.02)	4.16(0.02)	3.96(1.55)	3.70[d]
[7]CPP	S_1	2.61(0.02)	3.33(0.03)		3.04[b]
	S_2	3.42(0.00)	4.15(1.42)		
	S_3	3.50(0.01)	4.23(1.39)		
	S_4	3.62(1.04)	4.25(0.06)		
	S_5	3.69(1.02)	4.42(0.09)		3.65[d]
[9]CPP	S_1	2.93(0.02)	3.68(0.07)		3.14[c]
	S_2	3.51(0.06)	4.17(2.14)		
	S_3	3.55(1.47)	4.25(2.12)		
	S_4	3.56(0.02)	4.43(0.00)		
	S_5	3.61(1.20)	4.58(0.01)		3.65[d]

Note: CASSCF method involving the second-order strongly contracted n-electron valence state perturbation theory (SC-NEVPT2)

a. E. Kayahara, V. K. Patel, and S. Yamago, J. Am. Chem. Soc. 136, 2284,2014
b. P. Li, T. J. Sisto, E. R. Darzi, and R. Jasti, Org. Lett. 16, 182, 2014
c. N. Kubota, Y. Segawa, and K. Itami, J. Am. Chem. Soc. 137, 1356, 2015
d. E. J. Leonhardt and R. Jasti Nat. Rev. Chem. 3, 672, 2019
A.C. Kakarlamudi and S.R. Vennapusa J. Chem. Phys.,155, 044301, 2021

Estimation of the stabilization (or) reorganization energy

$$S_{min}/T_{min} = E_0^{(S/T)} - \frac{1}{2}\sum_{i}^{\alpha}\frac{\kappa_i^2}{\omega_i}$$

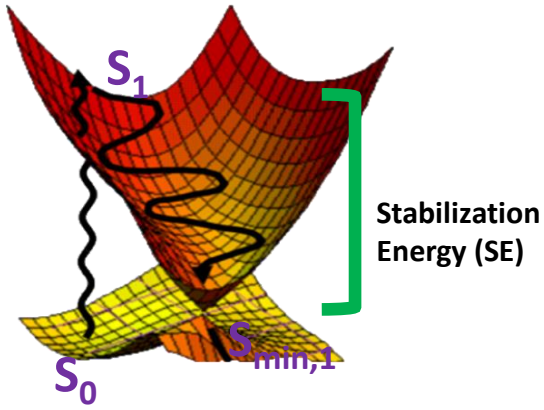

TABLE 2. Energetic minimum of S_1 and T_1 states of CPPs. The stabilization (or) reorganization energy of respective electronic state estimated by the LVC approach and TDDFT optimization calculation is given in the parenthesis. All values are in eV.

n in [n]CPP	Experiment		LVC		TDDFT Opt.	TDDFT Opt. literature [a]	
	$S_{min,1}$	$T_{min,1}$	$S_{min,1}$	$T_{min,1}$	$S_{min,1}$	$S_{min,1}$	$T_{min,1}$
5	-	-	1.30(0.71)	0.82(0.62)	1.38(0.63)	1.27	1.50
7	2.11 [b]	-	2.03(0.58)	1.59(0.44)	2.06(0.55)	2.20	2.09
9	2.51 [c]	1.96 [d]	2.43(0.50)	1.90(0.41)	2.48(0.46)	2.67	2.26

a. J. Liu, L. Adamska, S. K. Doorn, and S. Tretiak, Phys. Chem. Chem. Phys.17, 14613, 2015
b. T. J. Sisto, M. R. Golder, E. S. Hirst, and R. Jasti, J. Am. Chem. Soc. 133, 15800, 2011
c. Segawa, A. Fukazawa, S. Matsuura, H. Omachi, S. Yamaguchi, S. Irle, and K. Itami, Org. Biomol.Chem.10, 5979, 2012
d. M. Fujitsuka, C. Lu, B. Zhuang, E. Kayahara, S. Yamago, and T. Majima, J. Phys. Chem. A 123,4737, 2019
A.C. Kakarlamudi and S.R. Vennapusa J. Chem. Phys.,155, 044301, 2021

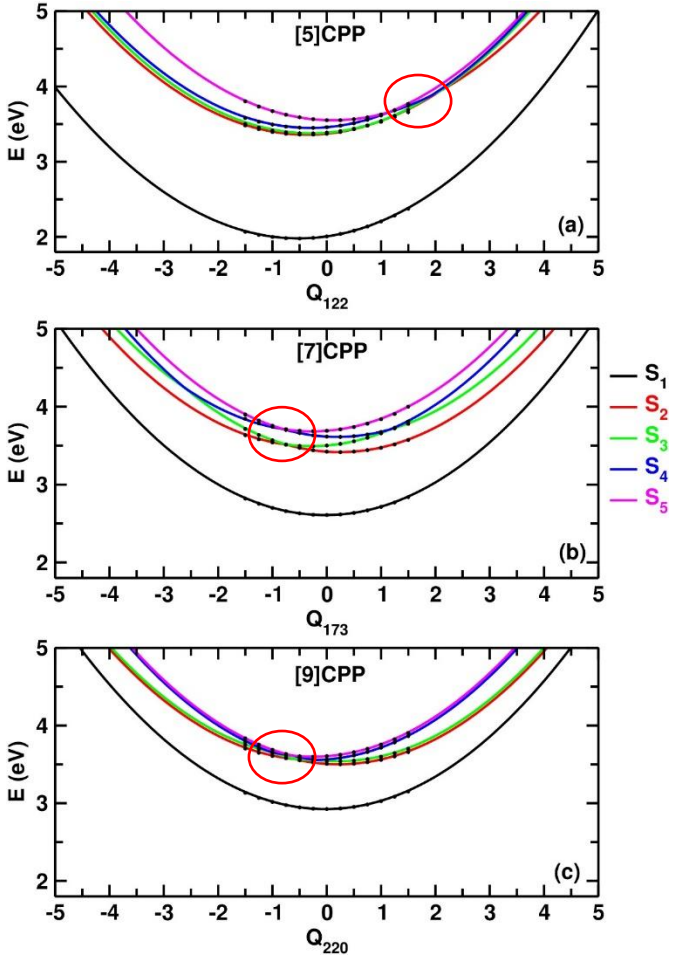

FIG. 3. Adiabatic potential energy cuts of low-lying singlet excited states of (a) [5]CPP, (b) [7]CPP, and (c) [9]CPP along the dimensionless normal coordinates of their respective C=C stretching mode. Computed ab initio vertical excitation energies (plus harmonic potential) are shown by the asterisks on each curve.

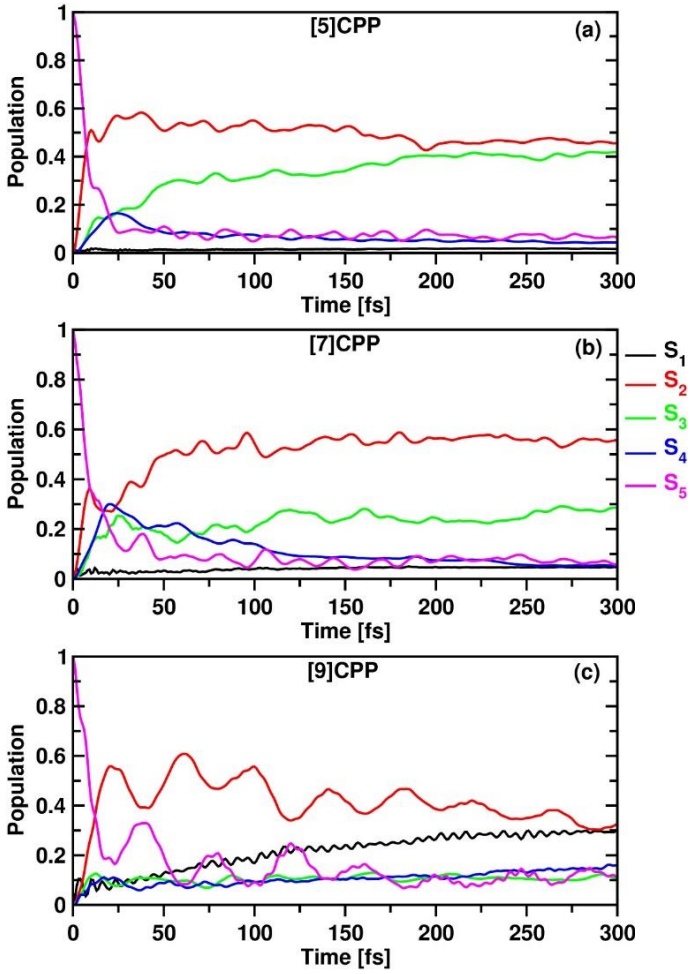

FIG. 4. Time-dependent diabatic electronic populations of singlet excited states generated by propagating the initial MCTDH wavepacket on S_5 of (a) [5]CPP, (b) [7]CPP, and (c) [9]CPP.

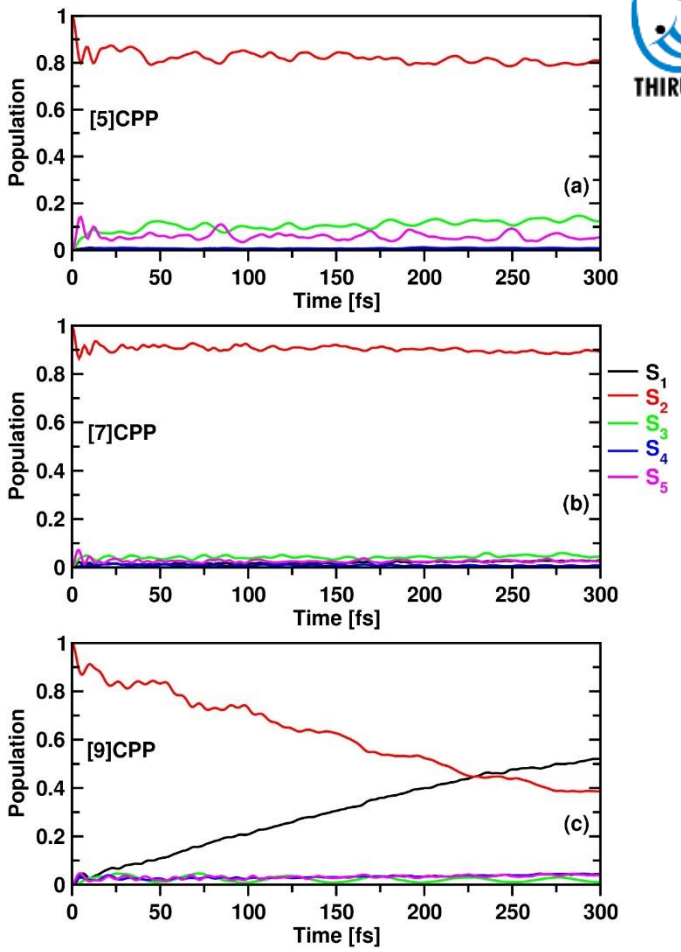

FIG. 5. Time-dependent diabatic electronic populations of singlet excited states generated by propagating the initial MCTDH wavepacket on S_2 of (a) [5]CPP, (b) [7]CPP, and (c) [9]CPP

Spin-orbit coupling(SOC) and ISC rates

Rate constant for ISC ($\mathbf{K_{ISC}^{nm}}$) is calculated using Fermi's golden rule where SOC values are obtained from PySOC code

$$K_{ISC}^{nm} = \frac{4\pi^2}{h} \rho_{FC} \left|\langle S_n|\hat{H}_{SOC}|T_m\rangle\right|^2$$

$\left|\langle S_n|\hat{H}_{SOC}|T_m\rangle\right|$ is the SOC-matrix element between the S_n and T_m states

ρ_{FC} denotes the Franck–Condon weighted density of states and is computed within the Marcus theory framework

$$\rho_{FC} = \frac{1}{\sqrt{4\pi\lambda'_M k_B T}} \exp\left[\frac{-(\Delta E_{ST} + \lambda'_M)^2}{4\lambda'_M k_B T}\right]$$

λ'_M, k_B, T, and ΔE_{ST} represent the Marcus-reorganization energy, Boltzmann constant, temperature, and adiabatic singlet–triplet energy gap, respectively

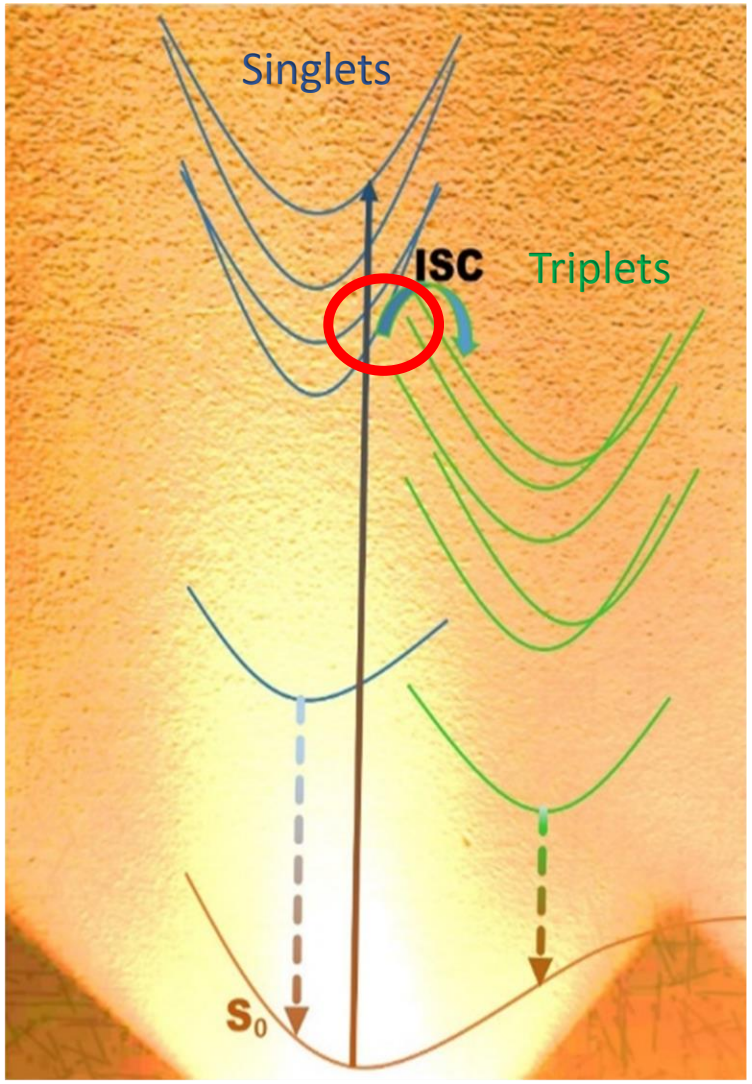

V. Lawetz, G. Orlandi, and W. Siebrand, J. Chem. Phys. 56, 4058, 1972
D. Beljonne, Z. Shuai, G. Pourtois, and J. L. Bredas, J. Phys. Chem. A 105, 3899, 2001
X. Gao, S. Bai, D. Fazzi, T. Niehaus, M. Barbatti, and W. Thiel, J. Chem. Theory Comput.13, 515, 2017

TABLE 3. Singlet-triplet energy difference (ΔS_1-T_n and ΔS_2-T_n) and associated spin-orbit coupling matrix elements (SOCMEs) computed using PySOC[a] at B3LYP/6-311G(d) level of theory for [5]-,[7]- and [9]CPP. SOCMEs are computed using the FC geometry of respective CPP.

[n]CPP	T_n	ΔS_1-T_n (cm^{-1})	SOC (cm^{-1})	K_{ISC} (s^{-1})	ΔS_2-T_n (cm^{-1})	SOC (cm^{-1})	K_{ISC} (s^{-1})
[5]CPP	T_6	10936.32	0.52	2.25E-43	69.37	0.51	1.81E+07
	T_5	9653.07	0.20	2.51E-34	1352.62	0.42	1.47E+05
	T_4	8890.05	0.11	1.75E-29	2115.64	0.55	5.70E+03
	T_3	3032.71	0.35	7.44E+00	7972.97	1.42	2.53E-21
	T_2	2963.35	0.32	1.02E+01	8042.34	0.41	7.83E-23
	T_1	171.80	0.02	2.45E+04	15582.18	0.45	4.18E-88
[7]CPP	T_6	6167.06	0.13	2.66E-13	394.41	0.03	1.84E+04
	T_5	4723.29	0.33	7.02E-06	1838.18	0.07	4.28E+02
	T_4	4712.00	0.33	7.69E-06	1849.47	0.07	3.83E+02
	T_3	657.36	0.12	1.79E+05	7218.83	0.7	1.89E-17
	T_2	1387.31	0.08	4.64E+03	7948.78	0.09	1.44E-23
	T_1	4658.77	0.03	7.85E-08	11220.24	0.15	9.38E-47
[9]CPP	T_6	4520.84	0.08	2.45E-06	171.80	0.01	6.35E+03
	T_5	862.23	0.12	9.03E+04	3830.42	0.08	1.08E-03
	T_4	671.88	0.11	1.39E+05	4020.77	0.05	9.48E-05
	T_3	2683.47	0.07	2.74E+00	7376.11	0.32	4.91E-19
	T_2	3286.78	0.05	2.43E-02	7979.43	0.03	9.22E-25
	T_1	5017.69	0.03	2.85E-09	9710.33	0.09	2.03E-35

$S_2 \rightarrow T_6$ for [5]CPP

$S_2 \rightarrow T_6$ for [7]CPP

$S_1 \rightarrow T_4$ for [9]CPP

a X. Gao, S. Bai, D. Fazzi, T. Niehaus, M. Barbatti, and W. Thiel, J. Chem. Theory Comput. 13, 515, 2017
A.C. Kakarlamudi and S.R. Vennapusa J. Chem. Phys.,155, 044301, 2021

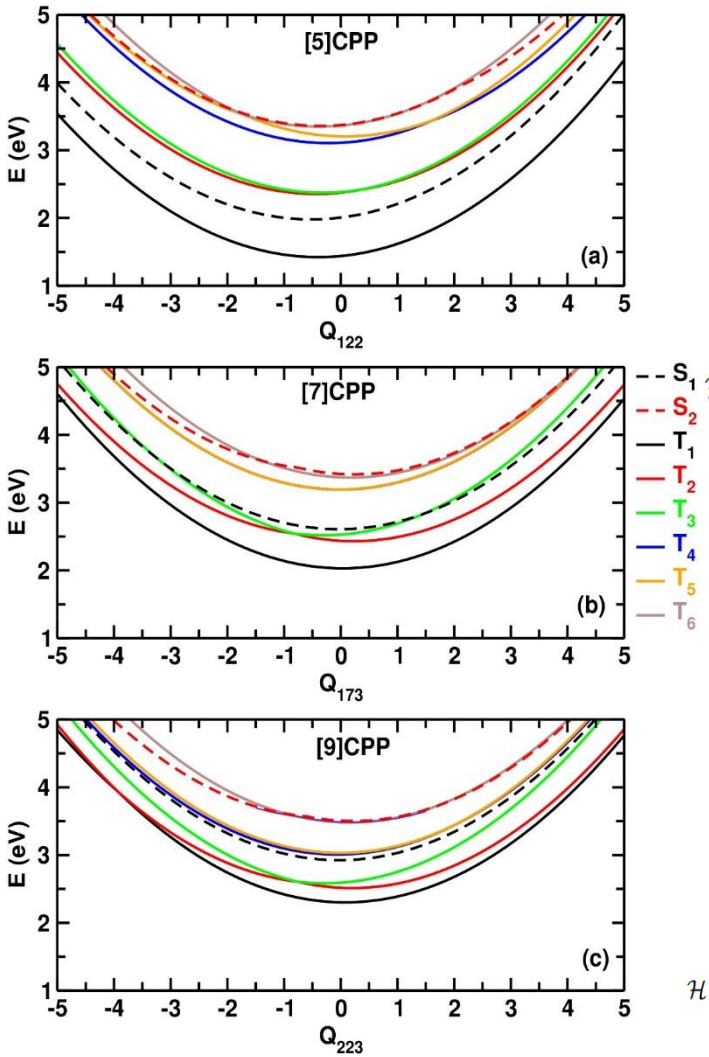

FIG. 6. Adiabatic potential energy cuts of low-lying excited states of (a) [5]CPP, (b) [7]CPP, and (c) [9]CPP along the dimensionless normal coordinates of their respective C=C stretching mode.

Hamiltonian to investigate the relaxation dynamics associated with S_2, S_3, S_4, S_5, T_4, T_5 and T_6 of [5]- and [7]CPP

$$\mathcal{H} = (\mathcal{T}_N+\mathcal{V}_0)\mathbf{1_7}+\begin{pmatrix} \mathbf{E}^0_{\mathbf{S}_2}+\sum_i \kappa_i^{(\mathbf{S}_2)}\mathbf{Q}_i & \sum_j \lambda_j^{(\mathbf{S}_2-\mathbf{S}_3)}\mathbf{Q}_j & \sum_j \lambda_j^{(\mathbf{S}_2-\mathbf{S}_4)}\mathbf{Q}_j & \sum_j \lambda_j^{(\mathbf{S}_2-\mathbf{S}_5)}\mathbf{Q}_j & \eta^{(\mathbf{S}_2-\mathbf{T}_4)} & \eta^{(\mathbf{S}_2-\mathbf{T}_5)} & \eta^{(\mathbf{S}_2-\mathbf{T}_6)} \\ & \mathbf{E}^0_{\mathbf{S}_3}+\sum_i \kappa_i^{(\mathbf{S}_3)}\mathbf{Q}_i & \sum_j \lambda_j^{(\mathbf{S}_3-\mathbf{S}_4)}\mathbf{Q}_j & \sum_j \lambda_j^{(\mathbf{S}_3-\mathbf{S}_5)}\mathbf{Q}_j & \eta^{(\mathbf{S}_3-\mathbf{T}_4)} & \eta^{(\mathbf{S}_3-\mathbf{T}_5)} & \eta^{(\mathbf{S}_3-\mathbf{T}_6)} \\ & & \mathbf{E}^0_{\mathbf{S}_4}+\sum_i \kappa_i^{(\mathbf{S}_4)}\mathbf{Q}_i & \sum_j \lambda_j^{(\mathbf{S}_4-\mathbf{S}_5)}\mathbf{Q}_j & \eta^{(\mathbf{S}_4-\mathbf{T}_4)} & \eta^{(\mathbf{S}_4-\mathbf{T}_5)} & \eta^{(\mathbf{S}_4-\mathbf{T}_6)} \\ & & & \mathbf{E}^0_{\mathbf{S}_5}+\sum_i \kappa_i^{(\mathbf{S}_5)}\mathbf{Q}_i & \eta^{(\mathbf{S}_5-\mathbf{T}_4)} & \eta^{(\mathbf{S}_5-\mathbf{T}_5)} & \eta^{(\mathbf{S}_5-\mathbf{T}_6)} \\ & & & & \mathbf{E}^0_{\mathbf{T}_4}+\sum_i \kappa_i^{(\mathbf{T}_4)}\mathbf{Q}_i & \sum_j \lambda_j^{(\mathbf{T}_4-\mathbf{T}_5)} & \sum_j \lambda_j^{(\mathbf{T}_4-\mathbf{T}_6)}\mathbf{Q}_j \\ & & & & & \mathbf{E}^0_{\mathbf{T}_5}+\sum_i \kappa_i^{(\mathbf{T}_5)}\mathbf{Q}_i & \sum_j \lambda_j^{(\mathbf{T}_5-\mathbf{T}_6)}\mathbf{Q}_j \\ h.c. & & & & & & \mathbf{E}^0_{\mathbf{T}_6}+\sum_i \kappa_i^{(\mathbf{T}_6)}\mathbf{Q}_i \end{pmatrix}$$

Hamiltonian to investigate the relaxation dynamics associated with S_1, S_2, S_3, S_4, S_5, T_4, T_5 and T_6 of [9]CPP

$$\mathcal{H} = (\mathcal{T}_N+\mathcal{V}_0)\mathbf{1_8}+\begin{pmatrix} \mathbf{E}^0_{\mathbf{S}_1}+\sum_i \kappa_i^{(\mathbf{S}_1)}\mathbf{Q}_i & \sum_j \lambda_j^{(\mathbf{S}_1-\mathbf{S}_2)}\mathbf{Q}_j & \sum_j \lambda_j^{(\mathbf{S}_1-\mathbf{S}_3)}\mathbf{Q}_j & \sum_j \lambda_j^{(\mathbf{S}_1-\mathbf{S}_4)}\mathbf{Q}_j & \sum_j \lambda_j^{(\mathbf{S}_1-\mathbf{S}_5)}\mathbf{Q}_j & \eta^{(\mathbf{S}_1-\mathbf{T}_4)} & \eta^{(\mathbf{S}_1-\mathbf{T}_5)} & \eta^{(\mathbf{S}_1-\mathbf{T}_6)} \\ & \mathbf{E}^0_{\mathbf{S}_2}+\sum_i \kappa_i^{(\mathbf{S}_2)}\mathbf{Q}_i & \sum_j \lambda_j^{(\mathbf{S}_2-\mathbf{S}_3)}\mathbf{Q}_j & \sum_j \lambda_j^{(\mathbf{S}_2-\mathbf{S}_4)}\mathbf{Q}_j & \sum_j \lambda_j^{(\mathbf{S}_2-\mathbf{S}_5)}\mathbf{Q}_j & \eta^{(\mathbf{S}_2-\mathbf{T}_4)} & \eta^{(\mathbf{S}_2-\mathbf{T}_5)} & \eta^{(\mathbf{S}_2-\mathbf{T}_6)} \\ & & \mathbf{E}^0_{\mathbf{S}_3}+\sum_i \kappa_i^{(\mathbf{S}_3)}\mathbf{Q}_i & \sum_j \lambda_j^{(\mathbf{S}_3-\mathbf{S}_4)}\mathbf{Q}_j & \sum_j \lambda_j^{(\mathbf{S}_3-\mathbf{S}_5)}\mathbf{Q}_j & \eta^{(\mathbf{S}_3-\mathbf{T}_4)} & \eta^{(\mathbf{S}_3-\mathbf{T}_5)} & \eta^{(\mathbf{S}_3-\mathbf{T}_6)} \\ & & & \mathbf{E}^0_{\mathbf{S}_4}+\sum_i \kappa_i^{(\mathbf{S}_4)}\mathbf{Q}_i & \sum_j \lambda_j^{(\mathbf{S}_4-\mathbf{S}_5)}\mathbf{Q}_j & \eta^{(\mathbf{S}_4-\mathbf{T}_4)} & \eta^{(\mathbf{S}_4-\mathbf{T}_5)} & \eta^{(\mathbf{S}_4-\mathbf{T}_6)} \\ & & & & \mathbf{E}^0_{\mathbf{S}_5}+\sum_i \kappa_i^{(\mathbf{S}_5)}\mathbf{Q}_i & \eta^{(\mathbf{S}_5-\mathbf{T}_4)} & \eta^{(\mathbf{S}_5-\mathbf{T}_5)} & \eta^{(\mathbf{S}_5-\mathbf{T}_6)} \\ & & & & & \mathbf{E}^0_{\mathbf{T}_4}+\sum_i \kappa_i^{(\mathbf{T}_4)}\mathbf{Q}_i & \sum_j \lambda_j^{(\mathbf{T}_4-\mathbf{T}_5)}\mathbf{Q}_j & \sum_j \lambda_j^{(\mathbf{T}_4-\mathbf{T}_6)}\mathbf{Q}_j \\ & & & & & & \mathbf{E}^0_{\mathbf{T}_5}+\sum_i \kappa_i^{(\mathbf{T}_5)}\mathbf{Q}_i & \sum_j \lambda_j^{(\mathbf{T}_5-\mathbf{T}_6)}\mathbf{Q}_j \\ h.c. & & & & & & & \mathbf{E}^0_{\mathbf{T}_6}+\sum_i \kappa_i^{(\mathbf{T}_6)}\mathbf{Q}_i \end{pmatrix}$$

A.C. Kakarlamudi and S.R. Vennapusa J. Chem. Phys.,155,044301, 2021

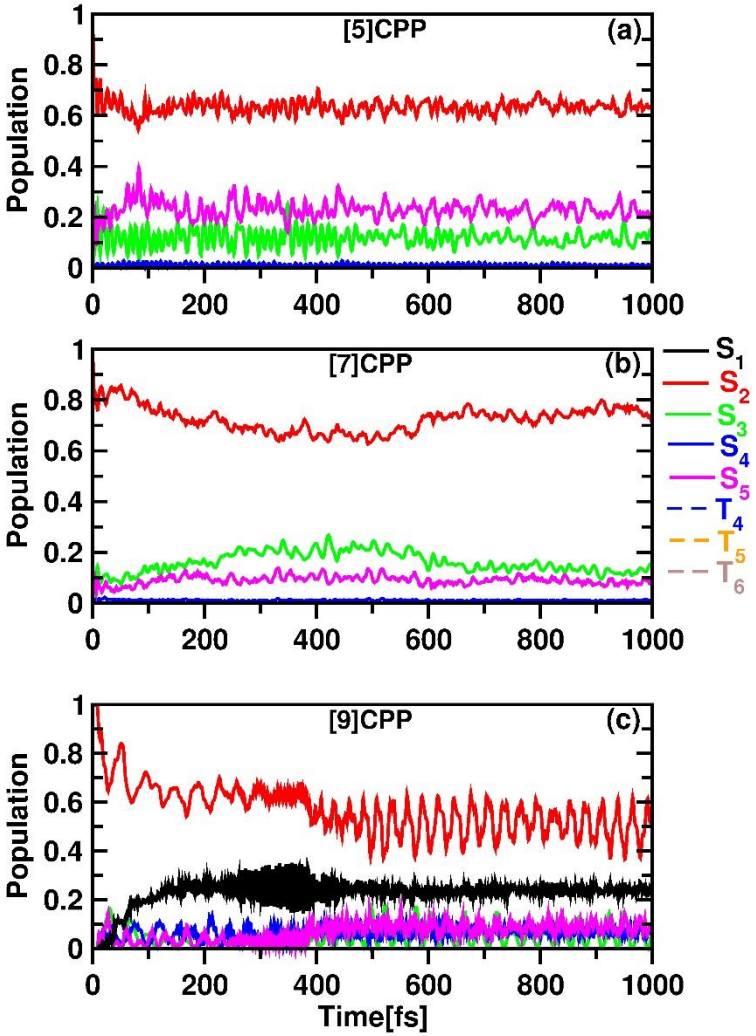

FIG. 7. Time-dependent diabatic electronic populations of singlet and triplet excited states generated by propagating the initial ML-MCTDH wavepacket on S_2 of (a) [5]CPP, (b) [7]CPP, and (c) [9]CPP. The Hamiltonian employed for the ML-MCTDH calculation contains the spin–orbit coupling constants of relevant singlet and triplet states

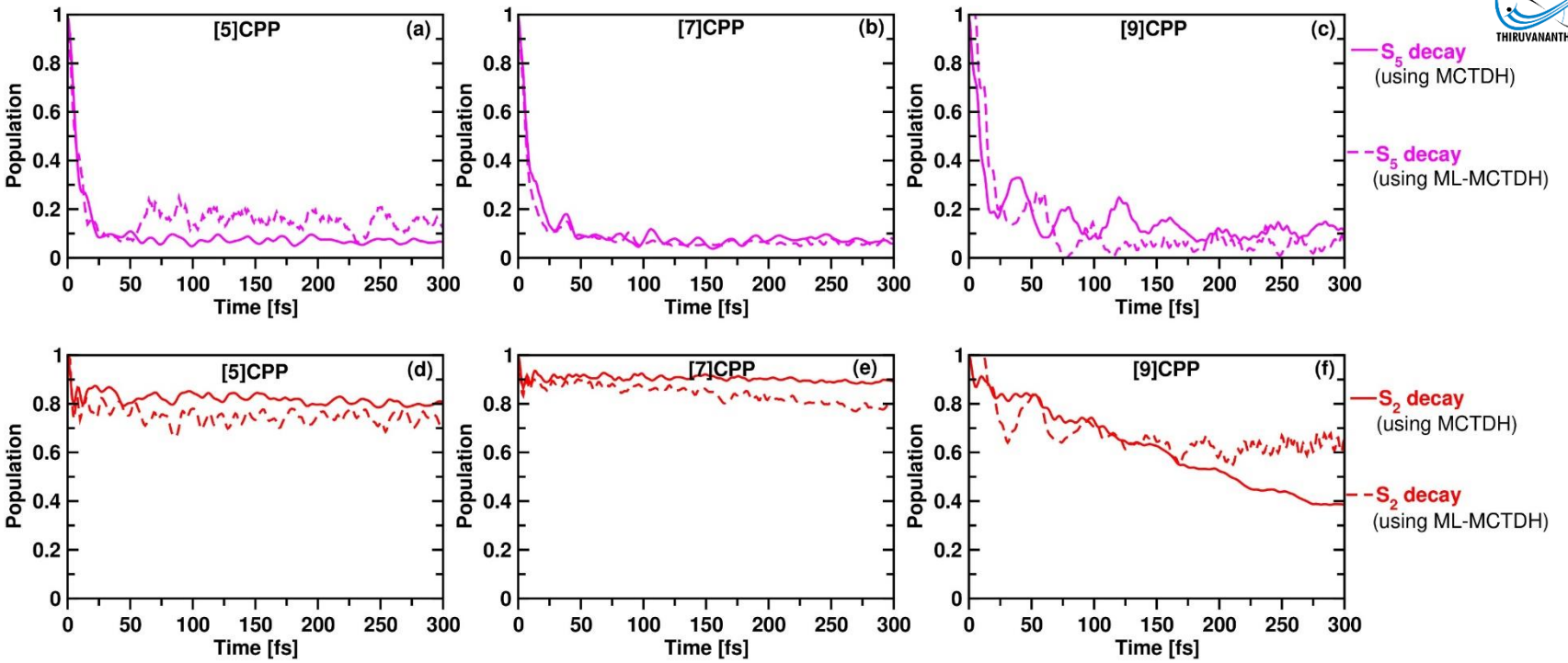

FIG. 8. Time-dependent diabatic electronic populations of singlet excited states generated by propagating the initial ML-MCTDH and MCTDH wavepacket on S_5 and S_2 of (a and d) [5]CPP, (b and e) [7]CPP, and (c and f) [9]CPP.

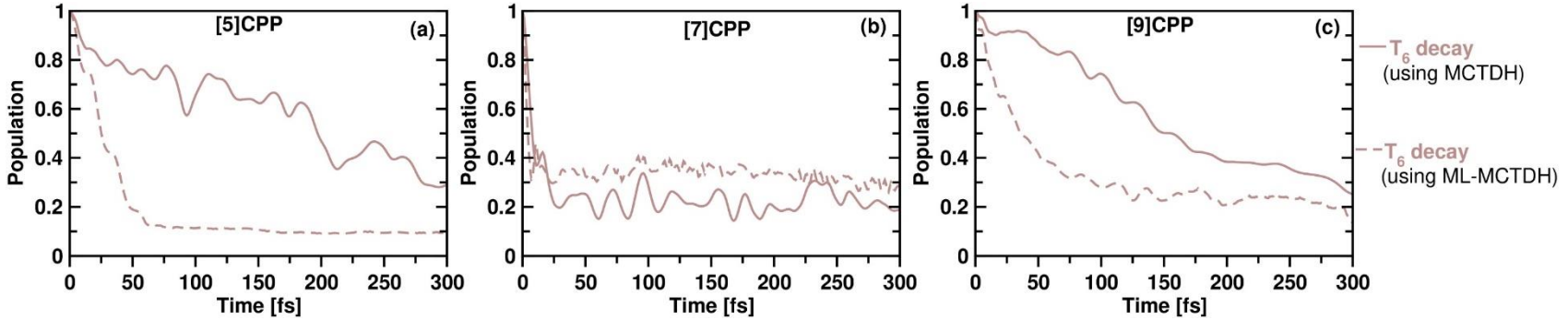

FIG. 9. Time-dependent diabatic electronic populations of triplet excited states generated by propagating the initial ML-MCTDH and MCTDH wavepacket on T_6 of (a) [5]CPP, (b) [7]CPP, and (c) [9]CPP.

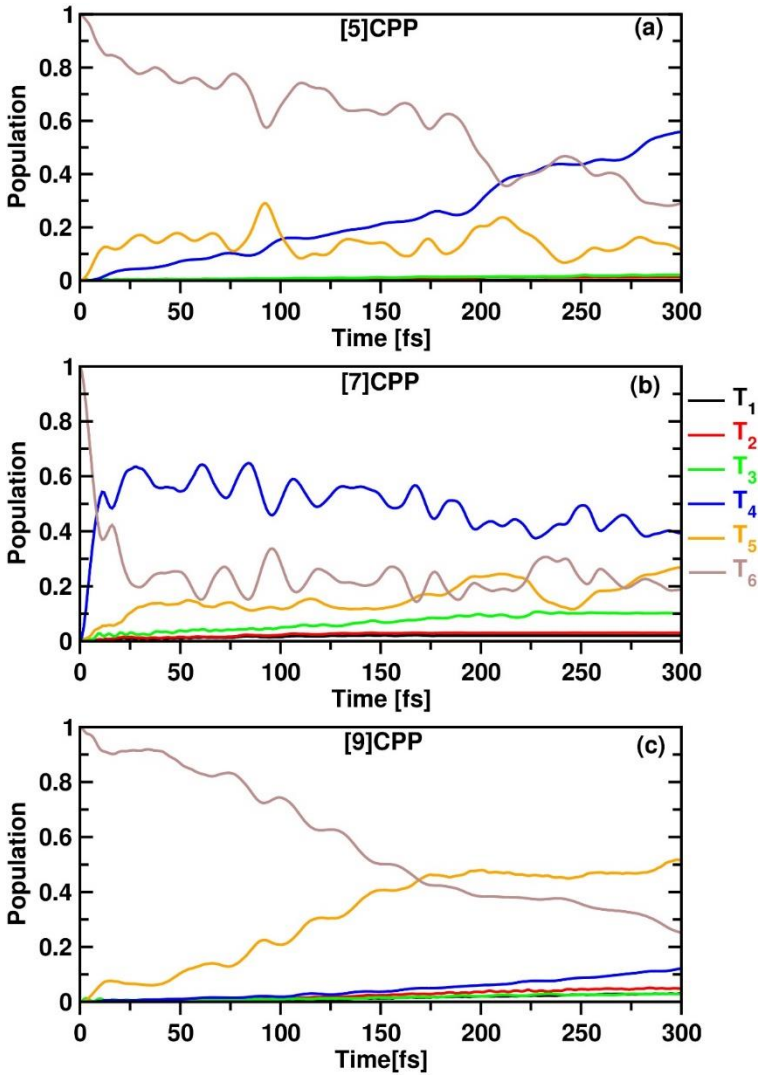

FIG. 10. Time-dependent diabatic electronic populations of triplet excited states generated by propagating the initial MCTDH wavepacket on T_6 of (a) [5]CPP, (b) [7]CPP, and (c) [9]CPP.

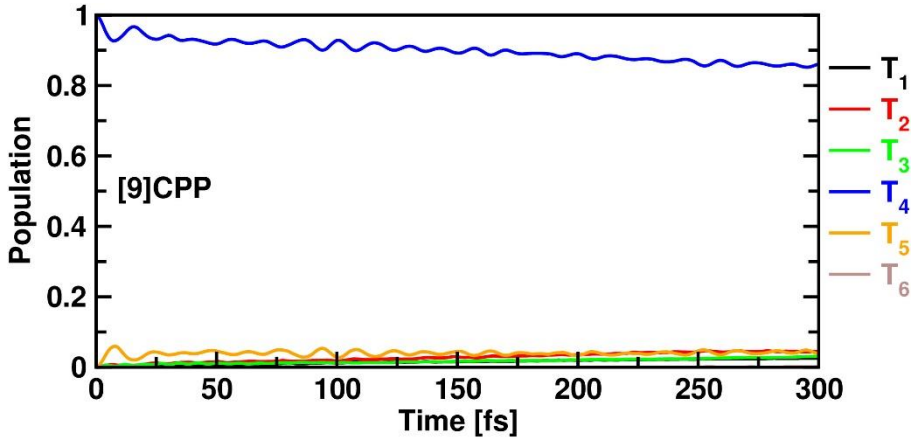

FIG. 11. Time-dependent diabatic electronic populations of triplet excited states generated by propagating the initial MCTDH wavepacket on T_4 of [9]CPP.

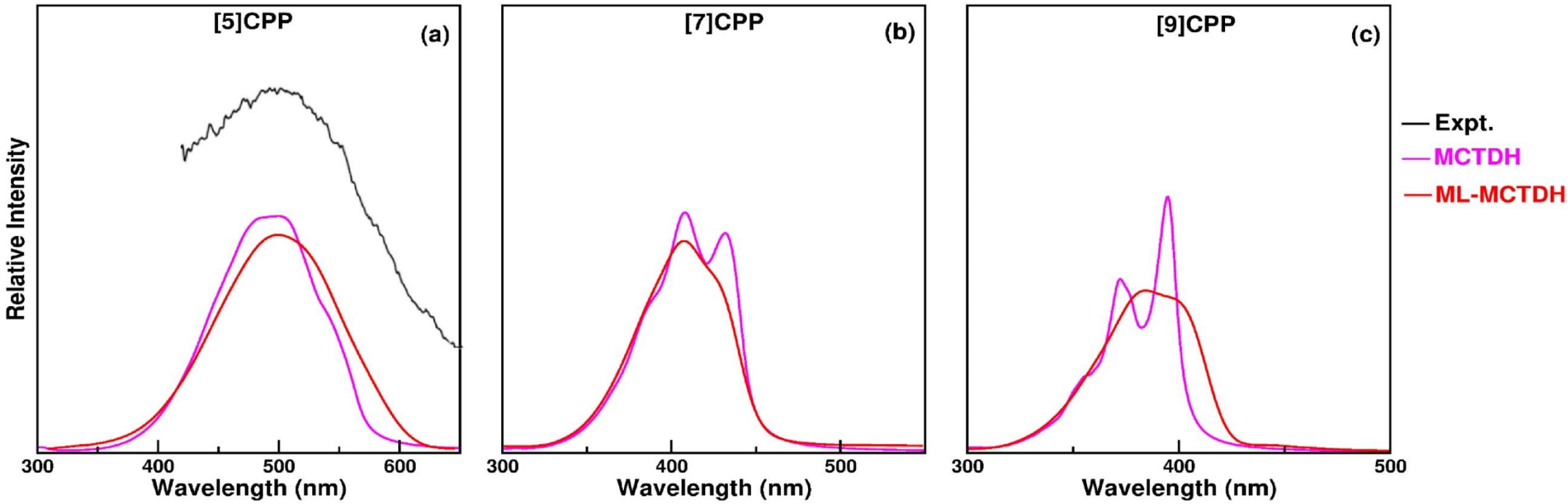

FIG. 12. The theoretical S_1 absorption spectrum of a) [5]CPP b) [7]CPP and [9]CPP. The MCTDH wavepacket dynamics simulations are performed using relevant 26 vibrational DOFs, whereas the ML-MCTDH method employs full-dimensionality of CPP. The experimental spectrum of [5]CPP is reproduced from Ref. [a]

a. E. Kayahara, V. K. Patel, and S. Yamago, J. Am. Chem. Soc. 136, 2284-2287, 2014
A.C. Kakarlamudi and S.R. Vennapusa J. Chem. Phys.,155, 044301, 2021

Conclusion

- We perform a combined analysis of energetics and SOC constants
- Wavepacket dynamics reveal an ultrafast $S_5 \rightarrow S_2$ IC in all these molecules
- Hence ISC pathways more likely from S_2 state, with T_6 being the receiver state
- On the other hand for [9]CPP, the $S_1 \rightarrow T_4$ ISC happens after a rapid $S_2 \rightarrow S_1$ IC decay
- Experimental fluorescence and phosphorescence emission energies are well reproduced with the LVC framework employed in this study

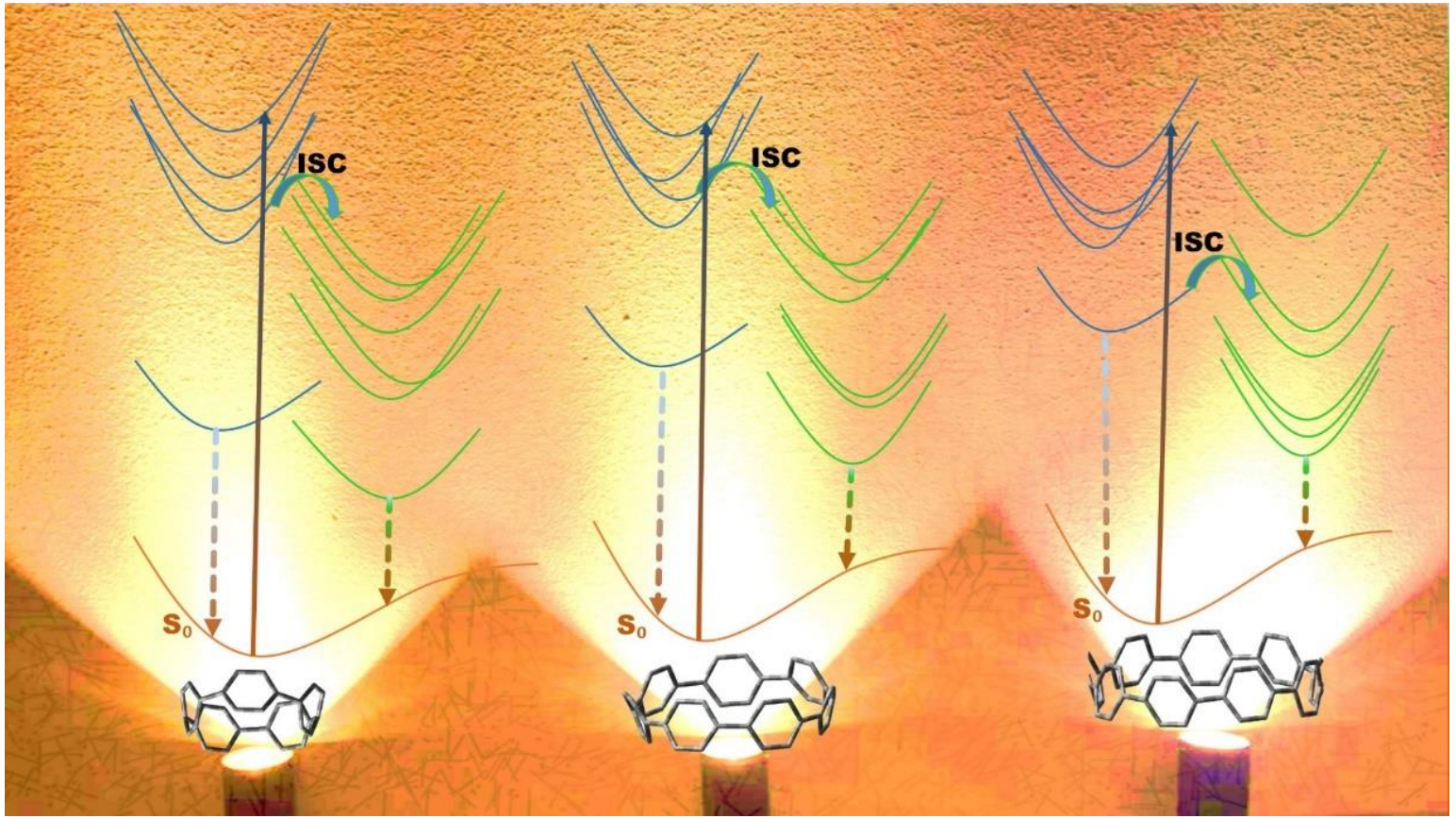

Acknowledgement

Dr Vennapusa Sivaranjana Reddy

All the Faculty members of IISER-TVM

All my lab mates

Friends and Family members

IISER THIRUVANANTHAPURAM

MHRD GOVERNMENT OF INDIA

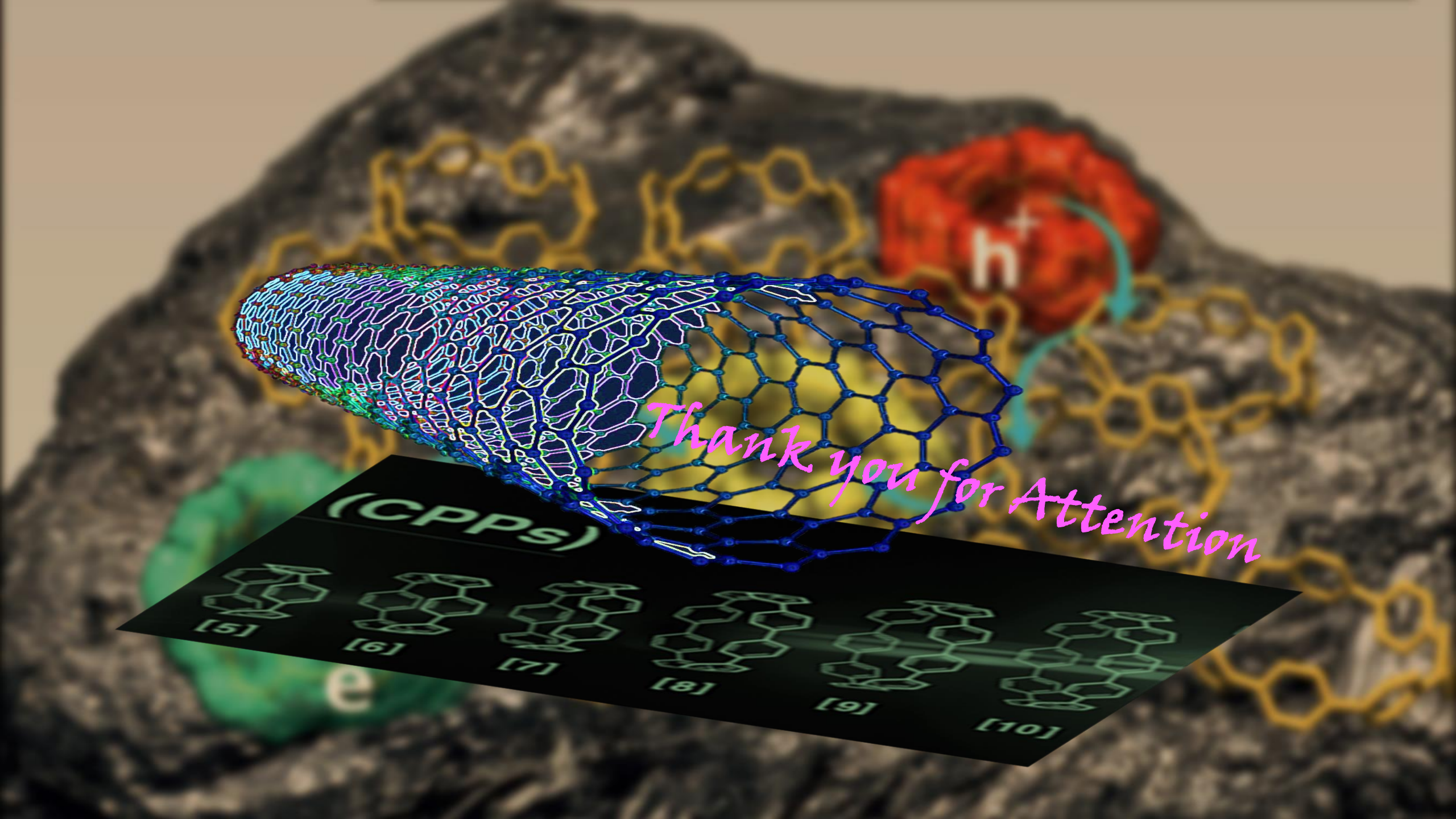
h+
e
(CPPs)
[5]
[6]
[7]
[8]
[9]
[10]
Thank you for Attention